DOI 10.1007/s11182-014-0323-6

Russian Physics Journal, Vol. 57, No. 7, November, 2014 (Russian Original No. 7, July, 2014)

PHYSICS OF SEMICONDUCTORS AND DIELECTRICS

MULTI-RELAXATION TEMPERATURE-DEPENDENT DIELECTRIC MODEL OF THE ARCTIC SOIL AT POSITIVE TEMPERATURES

I. V. Savin[1] and V. L. Mironov[1,2,3]

UDC 537.226.8

Frequency spectra of the dielectric permittivity of the Arctic soil of Alaska are investigated with allowance for the dipole and ionic relaxation of molecules of the soil moisture at frequencies from 40 MHz to 16 GHz and temperatures from –5 to +25°C. A generalized temperature-dependent multi-relaxation refraction dielectric model of the humid Arctic soil is suggested.

Keywords: dielectric permittivity, humid soils, spectroscopic parameters, Maxwell–Wagner relaxation.

INTRODUCTION

Nowadays microwave satellite radar sensing allows the soil cover to be monitored in the vast Arctic region. However, to monitor the permafrost state, dependences of the dielectric constant of soil on its humidity and temperature must be known. The generalized refraction dielectric model for the frequency spectra of humid soils (GRDMHS) suggested in [1] became the effective tool for prediction of dielectric spectra of humid soils in the microwave range. Then the generalized refraction dielectric model of the humid Arctic soil has been developed in [2, 3] on its basis. These models consider only the dipole relaxation of moisture molecules in gigahertz frequency range and can be called single-relaxation GRDMHS. Errors in prediction of dielectric properties using the models based on the single-relaxation GRDMHS [2–4] appear much less than those for the traditionally employed semi-empirical dielectric model suggested in [5]. Meanwhile, errors of dielectric models [2–4] considerably increase when the frequency decreases below 1.0 GHz. This is due to the fact that they do not take into account a considerable increase in the real and imaginary parts of the complex dielectric permittivity (CDP) of humid soils observed in experiments [6, 7] in megahertz frequency range. In [7] it has been demonstrated that this increase can be caused by the Maxwell–Wagner ionic relaxation [8] in bound and film soil moistures.

In the present work a temperature multi-relaxation GRDM model of the humid Arctic soil is developed with allowance for both dipole and ionic relaxations of soil moisture molecules for frequencies from 40 MHz to 16 GHz and temperatures from –5 to +25°C. The mineral soil composition is presented in Table 1. The error of the developed multi-relaxation GRDM is estimated.

[1]L. I. Kirensky Institute of Physics of the Siberian Branch of the Russian Academy of Sciences, Krasnoyarsk, Russia; [2]Siberian State Aerospace University Named after Academician M. F. Reshetnev, Krasnoyarsk, Russia; [3]National Research Tomsk State University, Tomsk, Russia, e-mail: rsd@ksc.krasn.ru. Translated from Izvestiya Vysshikh Uchebnykh Zavedenii, Fizika, No. 7, pp. 41–47, July, 2014. Original article submitted December 30, 2013.

TABLE 1. Mineral Composition of the Examined Soil

Mineral composition	Content, %	Mineral composition	Content, %
Organics	80–90	Plagioclase	0.75
Calcite	4.5	Mica	0.75–1.5
Quartz	7.5–8.2	Smectite	0.75

DETERMINATION OF THE PARAMETERS OF THE MULTI-RELAXATION GRDM

Mironov *et al*. [9] developed a procedure for determining the parameters of dielectric spectra of multi-relaxation GRDM on the example of clayey chernosem. In this work, the same procedure is applied to the Arctic soil.

Laboratory measurements of the CDP spectra for humid Arctic soil were performed at frequencies from 40 MHz to 16 GHz and temperatures from +25 to –5°C in the regime of sample cooling. The temperature regime was provided with an Espec SU-241 heat/cold chamber. For CDP measurements, a Rohde&Schwarz vector chain analyzer ZVK was used that measured the parameters of the scattering matrix of a connected coaxial container with a soil sample. The CDP spectra were determined using the parameters of the scattering matrix. In this case, for frequencies from 40 MHz to 1 GHz and from 1 to 16 GHz, the procedures described in [10, 11], respectively, were used.

Furthermore, expressing the real, n_s, and imaginary, κ_s, parts of the complex refractive index (CRI) of humid soil as functions of the bulk moisture M relative to the weight of the dry sample, for the refractive dielectric model of the mixture [1] we obtain

$$\frac{n_s(M,f,t)-1}{\rho_d}=\begin{cases}\dfrac{n_m-1}{\rho_m}+\left(n_b(f,t)-1\right)M, & 0\le M\le M_t,\\ \dfrac{n_s(M_{t1},f,t)-1}{\rho_d}+\left(n_t(f,t)-1\right)\left(M-M_{t1}\right), & M_{t1}\le M\le M_{t2},\\ \dfrac{n_s(M_{t2},f,t)-1}{\rho_d}+\left(n_u(f,t)-1\right)\left(M-M_{t2}\right), & M\ge M_{t2},\end{cases} \tag{1}$$

$$\frac{\kappa_s(M,f,t)-1}{\rho_d}=\begin{cases}\dfrac{\kappa_m}{\rho_m}+\kappa_b(f,t)\,M, & 0\le M\le M_{t1},\\ \dfrac{\kappa_s(M_{t1},f,t)}{\rho_d}+\kappa_t(f,t)\left(M-M_{t1}\right), & M_{t1}\le M\le M_{t2},\\ \dfrac{\kappa_s(M_{t2},f,t)}{\rho_d}+\kappa_u(f,t)\left(M-M_{t2}\right), & M\ge M_{t2}.\end{cases} \tag{2}$$

Here n_s, n_m, n_b, n_t, and n_u and κ_s, κ_m, κ_b, κ_t, and κ_u are the real and imaginary parts of the CRI, respectively; f and t designate the frequency of the electromagnetic field and the temperature, respectively; and ρ_d is the density of the dry residue of the sample normalized by the moisture density. The subscripts s, m, b, t, and u in Eqs. (1) and (2) and in the subsequent expressions designate the humid soil, organic-mineral soil component, and bound (adsorbed), loosely bound (film), and free (capillary) soil moisture, respectively. In turn, M_{t1} and M_{t2} designate maximum possible amount of bound moisture and maximum possible total amount of bound and film moisture in soil of a concrete type, respectively.

Figure 1 shows the dependence of the normalized refractive index $(n_s-1)/\rho_d$ and normalized absorption coefficient κ_s/ρ_d of the sample versus the bulk humidity M at the indicated frequencies and a temperature of 20°C. From

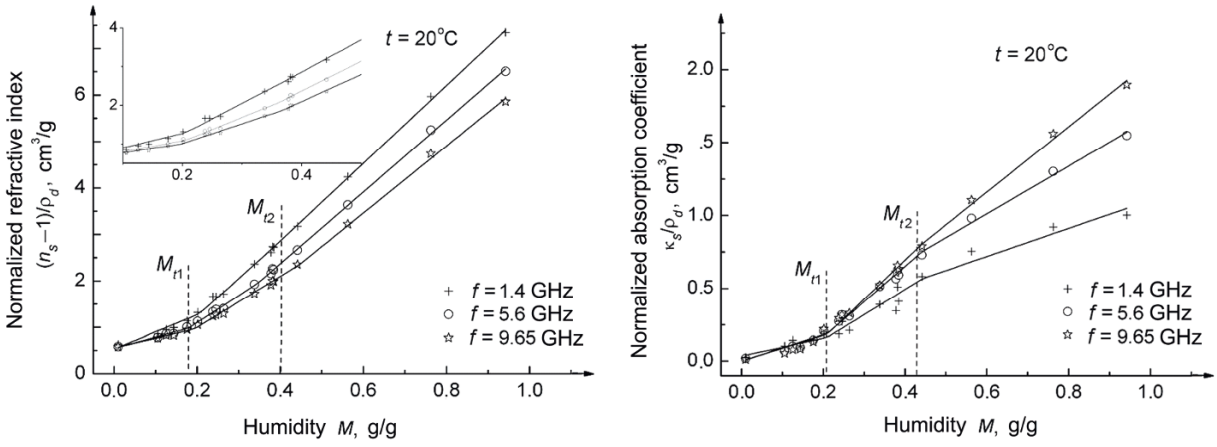

Fig. 1. Dependences of the normalized refractive index and normalized absorption coefficient on the soil humidity at a temperature of 20°C.

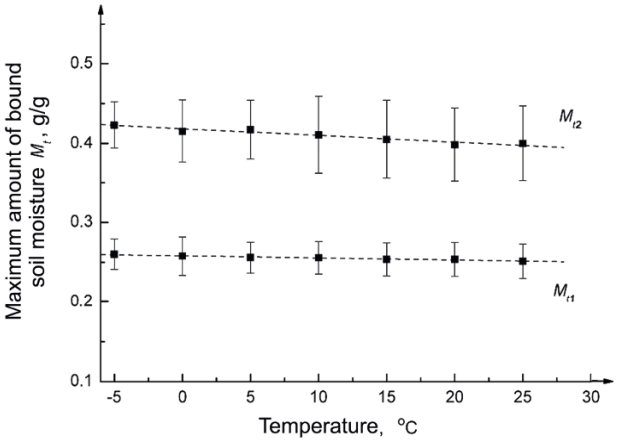

Fig. 2. Dependences of the maximum amount of tightly bound, M_{t1}, and bound, M_{t2}, moisture in the soil on the temperature.

the figure it can be seen that the entire set of points can be subdivided into three regions, namely, the region from $M = 0$ to $M = M_{t1}$ of the bound moisture, the region from $M = M_{t1}$ to $M = M_{t2}$ of the film moisture, and the region with M exceeding M_{t2} of the free soil moisture.

Figure 2 shows the dependences of the maximum amount of the bound moisture (M_{t1}) and total amount of the bound and film moisture (M_{t2}) in the sample on the temperature.

A regression analysis of the data shown in Fig. 2 yields expressions for the determination of the amount of bound and film moisture in the given sample at the given temperature:

$$M_{t1}(T) = 0.258 - 0.0003t(°\text{C}),\ -5°\text{C} \le t \le 25°\text{C},$$

$$M_{t2}(T) = 0.418 - 0.0008t(°\text{C}),\ -5°\text{C} \le t \le 25°\text{C}.$$

The real, n_p, and imaginary, κ_p, CRI components are expressed through the real, ε_p', and imaginary, ε_p'', CDP parts by the following formulas:

$$n_p\sqrt{2}=\sqrt{\sqrt{(\varepsilon'_p)^2+(\varepsilon''_p)^2}+\varepsilon'_p}\ ,\ \ \kappa_p\sqrt{2}=\sqrt{\sqrt{(\varepsilon'_p)^2+(\varepsilon''_p)^2}-\varepsilon'_p}\ , \tag{3}$$

where the subscript p takes values $p = s$, b, t, and u for the humid soil and the bound, film, and capillary moisture, respectively.

The real and imaginary CDP parts in Eqs. (3) for the soil moisture are described by the Debye equations [12] for non-conductive liquids which consider only the shear currents:

$$\varepsilon'_p=\frac{\varepsilon_{0pL}-\varepsilon_{0pM}}{1+\left(2\pi f\tau_{pL}\right)^2}+\frac{\varepsilon_{0pM}-\varepsilon_{0pH}}{1+\left(2\pi f\tau_{pM}\right)^2}+\ \frac{\varepsilon_{0pH}-\varepsilon_{\infty pH}}{1+\left(2\pi f\tau_{pH}\right)^2}+\varepsilon_{\infty pH}\ ,$$

$$\varepsilon''_p=\frac{\varepsilon_{0pL}-\varepsilon_{0pM}}{1+\left(2\pi f\tau_{pL}\right)^2}2\pi f\tau_{pL}\ +\frac{\varepsilon_{0pM}-\varepsilon_{0pH}}{1+\left(2\pi f\tau_{pM}\right)^2}2\pi f\tau_{pM}\ +\frac{\varepsilon_{0pH}-\varepsilon_{\infty pH}}{1+\left(2\pi f\tau_{pH}\right)^2}2\pi f\tau_{pH}\ . \tag{4}$$

Here ε_{0pL}, ε_{0pM}, and ε_{0pH} are low-frequency CDP limits, $\varepsilon_{\infty pH}$ is the high-frequency CDP limit, and τ_{pL}, τ_{pM}, or τ_{pH} are relaxation times for different relaxation types, respectively; all these parameters should be referred to the bound ($p = b$), film ($p = t$), and capillary ($p = u$) soil moisture; $\varepsilon_r = 8.854\cdot10^{-12}$ F/m is the dielectric permittivity of vacuum. To determine the CDP for the bound soil moisture, three-relaxation equation (4) must be used; the two-relaxation Debye equation which follows from Eq. (4) for $\varepsilon_{0uL} = \varepsilon_{0uM}$ must be used for the film soil moisture; at last, the single-relaxation Debye equation which follows from Eq. (4) for $\varepsilon_{0uL} = \varepsilon_{0uM} = \varepsilon_{0uH}$ must be used for the capillary soil moisture.

To calculate the CDP spectra for humid samples, we take advantage of the following formulas that consider both the shear currents using Eqs. (1)–(4) and the conduction currents using as a model parameters the ohmic conductivities of soil moistures:

$$\varepsilon'_s=n_s^2-\kappa_s^2,$$

$$\varepsilon''_s=\begin{cases}2n_s\kappa_s+\rho_d(M)M\sigma_b/2\pi f\varepsilon_r, & 0\le M\le M_{t1},\\ 2n_s\kappa_s+\rho_d(M)[M_{t1}\sigma_b+(M-M_{t1})\sigma_t]/2\pi f\varepsilon_r, & M_{t1}\le M\le M_{t2},\\ 2n_s\kappa_s+\rho_d(M)[M_{t1}\sigma_b+M_{t2}\sigma_t+(M-M_{t2})\sigma_u]/2\pi f\varepsilon_r, & M\ge M_{t2}.\end{cases} \tag{5}$$

Here σ_b, σ_t, and σ_u are the ohmic conductivities of the bound, film, and capillary soil moisture, respectively.

To determine the model parameters, it was suffice to use only a few spectra for humidities from 17 available ones. For this purpose, the CDP spectra for the chosen values of humidity were measured in the presence of only bound moisture, bound and film moistures, and all three types of soil moisture in the sample. In [2] the normalized real and imaginary CDP parts for the organic and mineral soil components $(n_m - 1)/\rho_m = 0.47$ and $\kappa_m/\rho_m = 0.006$ were determined that were required for the development of the model.

Furthermore, using the above-described procedure developed in [9] and the measured dielectric spectra shown in Fig. 3, the spectroscopic parameters of the bound, film, and capillary soil moistures were determined. The temperature dependences of the spectroscopic parameters are shown in Figs. 4–6.

Values of the parameters of the multi-relaxation model are presented in Table 2. In addition to the data presented in Table 2, the well-known value $\varepsilon_{\infty pH} = 4.9$ [1] was used. The dielectric spectra calculated with these parameters from formulas (1)–(5) are shown by the solid curves in Fig. 3. As can be seen from Table 2, the bound moisture in this case exhibits three relaxations rather than two, as previously described in [9]. This can be explained by the presence of two layers in the region of the bound moisture for the given soil, i.e., two types of moisture that differ by the dielectric properties, because the low-frequency relaxation (the Maxwell–Wagner relaxation) arises in inhomogeneous dielectrics when charge carriers are captured at the boundaries of the dielectric layers existing on the surfaces of films of moisture of different types.

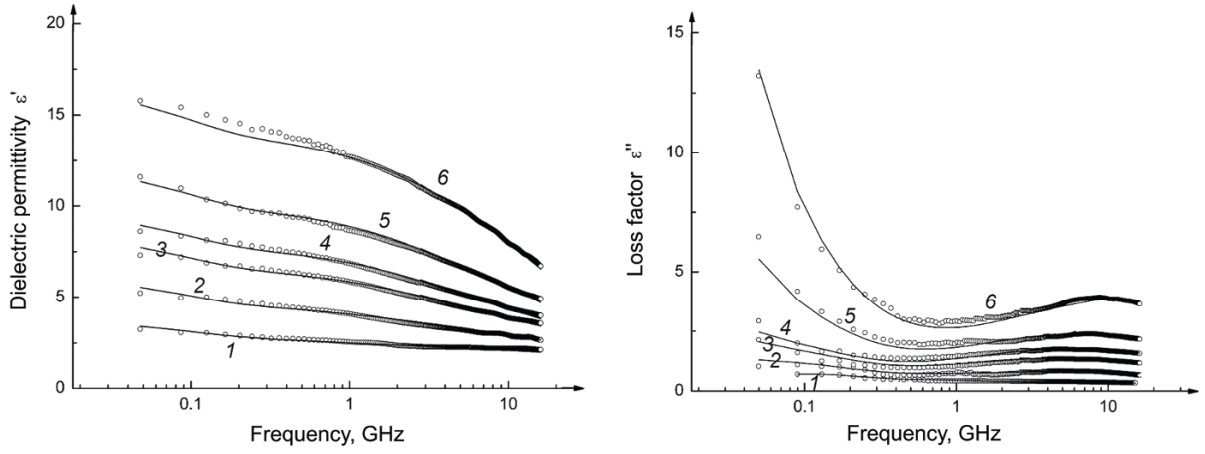

Fig. 3. Experimental spectra of the real and imaginary CDP parts (symbols) and results of their calculations with application of the GRDM (solid curves). The data are presented for the bulk moisture M (cm^3/cm^3) = 0.144 (curve *1*), 0.1764 (curve *2*), 0.264 (curve *3*), 0.338 (curve *4*), 0.442 (curve *5*), and 0.563 (curve *6*).

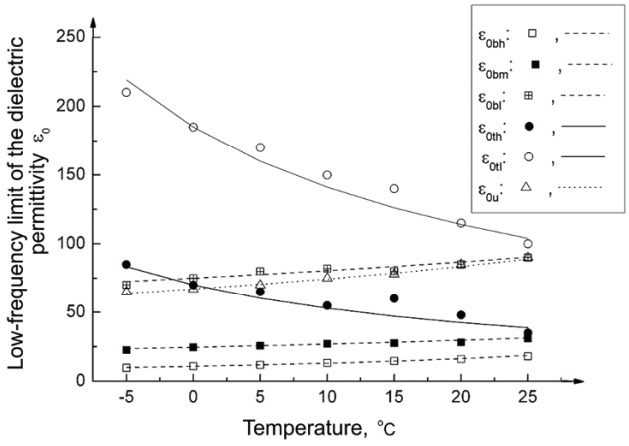

Fig. 4. Temperature dependences of the low-frequency limit of the dielectric permittivity for the soil moisture of the indicated types.

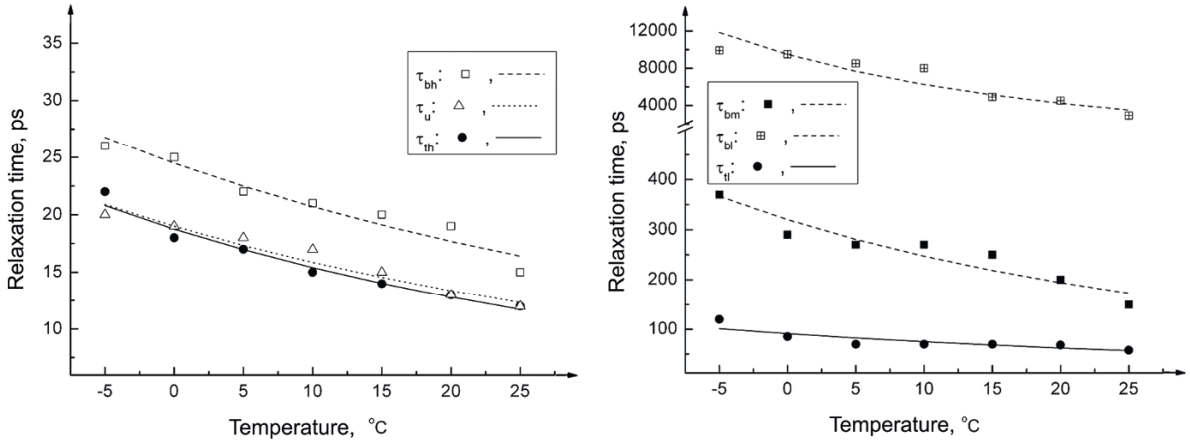

Fig. 5. Temperature dependences of the relaxation times for the soil moisture of the indicated types.

TABLE 2. Spectroscopic Parameters of the Multi-Relaxation Dielectric Model of the Examined Sample

Parameter	Measurement units	Bound moisture			Capillary moisture	Film moisture	
p	Subscripts	b			u	t	
Relaxation		1	2	3	1	1	2
$\varepsilon_{0p}(T_{s\varepsilon 0p})$	–	75	24.5	10.7	67	185	70
β_{v0p}	1/K	$+2.68\cdot10^{-3}$	$+1.03\cdot10^{-3}$	$+4.53\cdot10^{-3}$	$-5.93\cdot10^{-3}$	$-5.21\cdot10^{-4}$	$-1.36\cdot10^{-3}$
$T_{s\varepsilon 0p}$	°C	0	0	0	0	0	0
$\Delta H_p/R$	K	2957	1719	1020	1120	1234	1242
$\Delta S_p/R$	–	0.06	1.21	1.2	0.58	1.73	0.12
$\sigma_p(T_{s\sigma p})$	S/m	0			$+6.36\cdot10^{-3}$	$-2.32\cdot10^{-3}$	
$\beta_{\sigma p}$	(S/m)/K	0			0.18	0.08	
$T_{s\sigma p}$	°C	0			0	0	

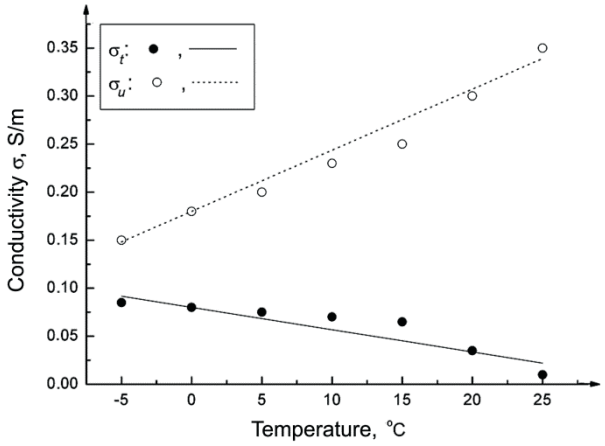

Fig. 6. Temperature dependences of the conductivity for the soil moistures of the indicated types.

Of special interest is the conductivity σ (see Fig. 6 and Table 2). For the bound moisture, it is close to zero, and this can imply that salts contained in the sample are insoluble in the bound moisture. In the film moisture the conductivity arises, but rather low. In capillary moisture, high conductivity is observed because of dissolution of various organic substances contained in the given soil.

ERROR OF THE MULTI-RELAXATION GRDMHS

Figure 7 shows the dependences of the measured CDP values on the calculated values of this quantity. The statistical error of CDP calculations was estimated based on the Pierson coefficient ρ and the standard deviation σ corresponding to the linear regressions (solid curves) for the data shown in Fig. 7. Values of the coefficients ρ and σ are given in Table 3. The linear regression equations that allow one to estimate the systematic error (the deviation of the regression line from the bisector) are also presented here. A comparison of the results presented here with an analysis of errors in [2, 3] demonstrates that the developed multi-relaxation GRDM can be used to calculate the CDP in the near-gigahertz and far megahertz frequency ranges with error smaller than that of the single-relaxation model.

TABLE 3. Estimates of the Errors of the Developed Multi-Relaxation Dielectric Model

Linear regression for ε'	$\varepsilon'_m = -0.048+1.02\cdot\varepsilon_p'$	Linear regression for ε''	$\varepsilon''_m = -0.022+1.015\cdot\varepsilon''_p$
ρ	0.999	ρ	0.997
σ	0.144	σ	0.151

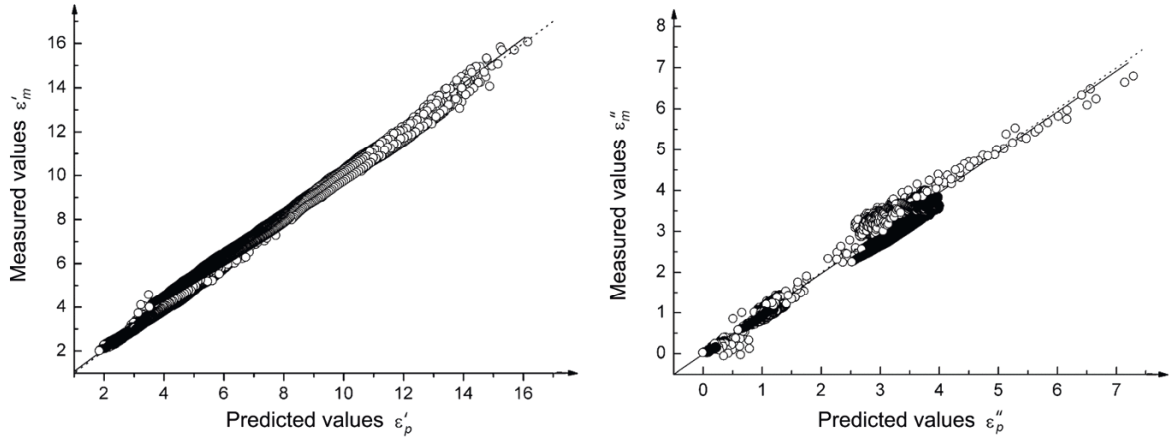

Fig. 7. Correlation between the predicted ε'_p, ε''_p and measured values ε'_m, ε''_m RP and CP (points). The dashed curves show the bisector (the ideal case of prediction without errors). The solid curve shows the linear regression line.

CONCLUSIONS

In this work, the temperature multi-relaxation GRDM has been constructed for the Arctic soil to calculate the CDP spectra at frequencies from 0.04 to 16 GHz and temperatures from –5 to +25°C, that is, the frequency range of the model is almost by two orders of magnitude wider in comparison with that of the single-relaxation model developed in [2]. Application of the single-relaxation model is limited by the range 1–16 GHz, since at frequencies below 1 GHz the errors of the model reach, as demonstrated by the experimental data, 300–400%. The errors of the suggested dielectric model based on the two- and three-relaxation spectra for the complex dielectric permittivity of film and bound moistures of the soil did not exceed the errors of experimental measurements in the entire frequency range. In addition, in this work it was demonstrated that three relaxations can be present in the bound soil moisture, which suggests the presence of the Maxwell–Wagner interlayer relaxation of two types, i.e., the presence in the soil of one more type of moisture. By analogy with [2], we further plan to expand the developed temperature multi-relaxation GRDMHS to encompass the negative temperatures.

REFERENCES

1. V. L. Mironov, M. C. Dobson, V. H. Kaupp, *et al*., IEEE Trans. Geosci. Remote Sens., **42**, No. 4, 773–785 (2004).
2. V. L. Mironov, R. D. De Roo, and I. V. Savin, IEEE Trans. Geosci. Remote Sens., **48**, No. 6, 2544–2556 (2010).
3. V. L. Mironov and I. V. Savin , Izv. Vyssh. Uchebn. Zaved., Fiz., **53**, No. 9/3, 241–246 (2010).

4. V. L. Mironov, L. G. Kosolapova, and S. V. Fomin, IEEE Trans. Geosci. Remote Sens., **47**, No. 7, Part 1, 2059–2070 (2009).
5. M. C. Dobson, F. T. Ulaby, M. T. Hallikainen, and M. A. El-Rayes, IEEE Trans. Geosci. Remote Sens., **23**, No. 1, 35–46 (1985).
6. J. O. Curtis, C. A. Weiss, Jr., and J. B. Everett, Technical Report EL-95-34, U.S. Army Corps Eng. Moistureways Exp. Station., Vicksburg (1995).
7. P. P. Bobrov, V. L. Mironov, O. V. Kondrat'eva, and A. V. Repin, in: Proc. XII Int. Conf. "Physics of Dielectrics," Vol. 1, Saint Petersburg (2011), pp. 207–209.
8. F. Kremer, A. Schonhals, and W. Luck, Broadband Dielectric Spectroscopy, Springer Verlag (2002).
9. V. L. Mironov, P. P. Bobrov, S. V. Fomin, and A. Yu. Karavaiskii, Russ. Phys. J., **56**, No. 3, 319–324 (2013).
10. M. P. Épov, P. P. Bobrov, V. L. Mironov, *et al*., Geol. Geofiz., **50**, No. 5, 613–618 (2009).
11. S. A. Komarov, V. L. Mironov, and Yu. I. Lukin, Russ. Phys. J., **49**, No. 9, 907–912 (2006).
12. Ya. Yu. Akhadov, Dielectric Properties of Pure Liquids [in Russian], Publishing House of Standards, Moscow (1972).
13. V. L. Mironov, P. P. Bobrov, L. G. Kosolapova, *et al*., in: Proc. of the International Geoscience and Remote Sensing Symposium IGARSS'06, Vol. 6, Denver (2006), pp. 2957–2961.